Determination of binding constants for strong complexation by affinity capillary electrophoresis: the example of complexes of ester betulin derivatives with (2-hydroxypropyl)-γ-cyclodextrin

Viktoria V. Sursyakova[1,*], Vladimir A. Levdansky[1], Anatoly I. Rubaylo[1,2,3]

[1]Institute of Chemistry and Chemical Technology SB RAS, Federal Research Center "Krasnoyarsk Science Center SB RAS", Akademgorodok 50/24, Krasnoyarsk, 660036, Russia

[2]Siberian Federal University, Svobodny pr. 79, Krasnoyarsk, 660041, Russia

[3]Federal Research Center "Krasnoyarsk Science Center SB RAS", Akademgorodok 50, Krasnoyarsk, 660036, Russia

∗Corresponding author.

Viktoria V. Sursyakova

E-mail: *viktoria_vs@list.ru*

Tel.: +73912907261; fax: +73912494108

ORCID: http://orcid.org/0000-0002-7088-7300 (V.V. Sursyakova)

Funding information This work was conducted within the framework of the budget project AAAA-A17-117021310221-7 for Institute of Chemistry and Chemical Technology SB RAS.

Conflict of interest The authors have no conflicts of interest to declare.

Electronic supplementary material The online version of this article (doi:) contains supplementary material, which is available to authorized users.

Abstract

Complexation plays an important role in many biological phenomena, the analysis of different samples, optimization of separation processes, and increasing the pharmacological activity of drugs. This paper discusses the features of using mobility shift affinity capillary electrophoresis for studying the strong complexation. Electrophoretic peaks for this case are often triangular. It was shown that the use of electrophoretic mobility obtained from the peak apex time in calculation of binding constants leads to significant systematic and random errors, and the parameter a_1 of the Haarhoff-Van der Linde function should be used instead of the apex time. Distorted triangular peaks with dips were shown to be observed at too high a ratio of analyte concentration in the sample to ligand concentration in the background electrolyte, and the peaks and parameter a_1 significantly shifted. It was found that the permissible excess of analyte concentration over ligand concentration is approximately 10-35, provided that the parameter a_1 is used, but the peak shape should be used as a landmark, and only triangular peaks without dips should be fitted with the function. The lowest possible analyte concentration should be utilized, which allows to use a wider range of ligand concentration leading to higher precision of determining the binding constants values. Kinetically labile 1:1 complexes between (2-hydroxypropyl)-γ-cyclodextrin (HP-γ-CD) and betulin 3,28-diphthalate (DPhB) and betulin 3,28-disuccinate (DScB) were studied as an example. The binding constants logarithms at 25 °C are 7.23 ± 0.03 and 7.13 ± 0.10 for the HP-γ-CD complexes of DPhB and DScB, respectively.

Keywords Betulin derivatives; Stability constants; Haarhoff-Van der Linde function; High-affinity interaction; Inclusion complexes; Electromigration dispersion

Introduction

Complexation is fundamental for understanding many biological phenomena. It is widely used in the analysis of different samples, optimization of separation processes, and increasing the pharmacological activity of drugs. For the latter purpose, inclusion or guest-host complexes, with cyclodextrins (CDs), natural macrocyclic molecules formed from residues of α-1,4-bonded D-glucopyranose [1, 2], are often used. Analytical methods to study CD complexes in aqueous solutions can be classified into separation techniques, such as affinity capillary electrophoresis (ACE) and high performance liquid chromatography (HPLC), and non-separation techniques (spectroscopic and electroanalytical techniques, polarimetry, isothermal titration calorimetry, etc) [3]. To determine binding constants, solutions with a fixed guest concentration and varying the concentration of the CD host are usually used in non-separation techniques. For strong complexation, it is necessary to use very low concentrations both for guest and host compounds in order to obtain the mole fractions of complexes significantly different from 1. For example, if

the binding constant is equal to 10^7 M^{-1}, then these concentrations are 0.1-10 μM, for more details see Electronic Supplementary Material, section S1. But a measured property, such as UV adsorption, conductivity, heat of chemical reactions, etc, in non-separation techniques is almost directly proportional to the guest and host concentrations, and sensitivity and precision of the techniques in this case fall greatly, if their usage is still possible. Whereas in ACE, which is a modern and rapid method with low reagent consumption [4-6], the measured effective electrophoretic mobility of a guest is almost independent of how small the guest concentration is used provided that guest is detectable at this concentration. HPLC, unlike to ACE, is not very convenient for studying CD complexes; CDs are chemically bound to the stationary phase, which is laborious, or CDs are added to the mobile phase [3], which leads to large CDs consumption. For hydrophobic guests, an organic solvent should be added to the mobile phase, and the values of binding constants obtained from HPLC are not directly comparable to those for aqueous solutions [3].

Mobility shift affinity capillary electrophoresis (ms ACE) is the most commonly used mode of ACE [7-27]. In this method, several electropherograms of the analyte injected as a sample are recorded using background electrolytes (BGE) with varying ligand content. For kinetically labile complexes, the analyte electrophoretic mobility depends on the mole fractions and ionic mobilities of all species into which the analyte can transform. The dependence of the effective electrophoretic mobility of the analyte for the case of 1:1 complexation on the ligand concentration in BGE is as follows:

$$v_i \cdot \mu_{eff,\ i} = \frac{\mu_D + \mu_{11} K_{11} [CD]_i}{1 + K_{11} [CD]_i} \quad (1)$$

where v_i is the coefficient allowing the corrections for the viscosity change, $\mu_{eff,\ i}$ is the effective electrophoretic mobility, μ_D and μ_{11} are the ionic mobilities of D and the complex D/CD, respectively, K_{11} is the binding (stability) constant of the complex D/CD, $[CD]_i$ is the CD concentration in BGE. To calculate the binding constant on the base of Eq. (1), a number of linearized equations can be used as well as a nonlinear regression fitting that is more accurate [28]. Dubský et al. suggested the CEval software that allows, besides evaluation of some peak parameters, to calculate binding constants using Eq. (1) by applying a nonlinear regression fitting [29] and that can be downloaded for free from http://echmet.natur.cuni.cz/. A number of parameters are of great importance to accurately determine the binding constants, among which one of the principal parameters for the CD complexes is data point range (DPR) [10]:

$$DPR = R_{C_n} - R_{C_1} \quad (2)$$

$$R_i = \frac{K_{11} [CD]_i}{1 + K_{11} [CD]_i} \quad (3)$$

where R_{C_n} and R_{C_1} are the mole fractions of the complexed analyte at the highest and lowest (nonzero) ligand concentration, respectively, R_i is the mole fraction of the complexed analyte at the ligand concentration in BGE equaled to $[CD]_i$. The accuracy and precision of ms ACE binding studies can be greatly improved by using at least five data points located at the upper part of the binding hyperbola with DPR > 0.4.

In ms ACE, the ligand concentration in BGE should be 10–100 times higher than the analyte concentration in the sample in order to the assumption that the ligand concentration in the sample zone is equal to the ligand concentration in BGE would be correct [25, 28]. However, for strong complexation, it can be impossible to record the electrophoretic peaks of analytes at such a low concentration, because the product $K_{11}[CD]_i$ is important. For example, in order to obtain mole fractions R_i from 0.5 to 0.95 (DPR > 0.4) for a system with log K = 6, as follows from Eq. (3), the ligand concentration range in BGE should be from 1 to 19 μM, and the analyte concentration in sample should be less than 0.1 μM. In addition, a narrow sample zone should be injected into capillary and the sample should be diluted with BGE to eliminate the stacking effect resulting to systematic errors due to a shift in the migration time [30]. This leads to the fact that ms ACE with the use of electrophoretic mobility calculated from the peak apex, as a rule, is applied to determine binding constants lower than 10000; the application of ms ACE for the determination of greater constants values is limited by the relatively low concentration sensitivity of detection [16, 31].

If the analyte concentration in the sample is higher than the ligand concentration in BGE, then triangular peaks are observed in electropherograms due to electromigration dispersion (EMD) [32-34]. For this case, EMD is a result of ligand deficiency in the sample zone in the initial time of electrophoretic separation. Though, ligand is being supplied into the sample zone during electrophoretic separation and is being consumed on the complex formation until the equilibrium ratio of complex concentration to analyte concentration has been achieved. Since this process is not instant and a ligand concentration gradient along the sample length is present, the sample zone broadens with shifting the concentration maximum toward one of the zone boundaries. The electrophoretic mobility of such zone shifts because in the initial time the zone moves with rate corresponding to a lower ligand concentration. The more the ligand deficiency and the lower the ligand concentration in BGE, the more time needed to achieve the equilibrium (the state when the ligand consumption in the sample zone stops) and the more extended peaks and the greater time shift.

Different approaches was suggested to take into account the effect of this phenomenon in the sample zone on the electrophoretic mobility, but the approaches are very complicated [5, 35]. In 2005, Le Saux et al. showed that if the electrophoretic mobility is calculated using the

parameter a_1 of the Haarhoff-Van der Linde (HVL) function instead of the migration time measured at the peak apex, then the effect of ligand deficiency on effective electrophoretic mobility can be eliminated [36, 37]:

$$f(t) = \frac{\frac{a_0 a_2}{a_1 a_3 \sqrt{2\pi}} \exp\left[-\frac{1}{2}\left(\frac{t-a_1}{a_2}\right)^2\right]}{\frac{1}{\exp\left(\frac{a_1 a_3}{a_2^2}\right)-1} + \frac{1}{2}\left[1+\mathrm{erf}\left(\frac{t-a_1}{\sqrt{2}a_2}\right)\right]} \quad (4)$$

where a_0 is the peak area, a_1 and a_2 are the peak center and standard deviation of the Gaussian part, respectively, a_3 is a measure of the peak distortion, t is the time, $\mathrm{erf}(x) = \frac{2}{\sqrt{\pi}}\int_0^x e^{-t^2} dt$ is the error function. The HVL function was taken from gas chromatography, and it is used in CE to calculate the true values of electrophoretic mobility at a high analyte concentration for triangular peaks due to electromigration dispersion [38, 39]. To fit peaks with the HVL function, the CEval software can be used [29].

Usually, the logarithms of binding constants for the CD complexes, log *K*, are in the range from 1 to 4 [40, 41]. The values of log *K* in the range of 4-7 are rare, including those obtained using ACE [8, 9, 17-20, 42-44]. Meanwhile, for log *K* > 3-4, fitting the electrophoretic peaks with the HVL function and calculating the electrophoretic mobility by the application of the a_1 parameter of this function were used only in studies [9, 18, 34]. The peaks in studies [8, 17, 20] seem symmetrical, which is possibly caused by the low analyte concentration and separation conditions applied. The peak shape is not discussed in paper [44], as well as in studies [19, 42, 43] in which electropherograms of the compounds under study are not shown.

In addition, it is interesting to know to what extent the analyte concentration in the sample (C_{an}) can be higher than the ligand concentration (C_L) in BGE ($r = C_{an}/C_L$) if the electrophoretic peaks is fitted with the HVL function and the electrophoretic mobility is calculated by application of the a_1 parameter of this function instead of the migration time from the peak apex. Little attention has been devoted to this problem. In paper [36], it was shown that for moderately strong complexation with log *K* ~ 2.6-2.8, a tenfold excess of analyte concentration over ligand concentration is allowed. However, for a strong complexation with log *K* ~ 4.4, this conclusion is not obvious due to the interference of the stacking effects [36]. Moreover, the peak shape at r > 10 has not been discussed. In short communication [9], it was mentioned that a large excess of analyte concentration in samples over ligand concentration in BGE leads to a strong distortion of the sample zone and the impossibility of the HVL function application, but this problem has not been studied in details.

It is also interesting to evaluate how significant errors in binding constants are obtained from the mobility calculated from the peak apex time relative to the binding constants obtained from the mobility calculated from the a_1 parameter. In paper [36], binding constants calculated in

two ways are compared, but precision in terms of the confidence interval (CI) or standard deviation for binding constants isn't given so that it is difficult to evaluate significance of the difference in these values. To our knowledge, there are no other comparisons for such cases in the literature.

The aim of this paper was to consider the features of using ms ACE for studying the strong complexation and, in particular, to investigate the effect of excess of the analyte concentration in samples over the ligand concentration in BGE on the peaks shape and position, and possibility of using the HVL function for fitting such peaks. The complexation of ester betulin derivatives, betulin 3,28-diphthalate (DPhB) and betulin 3,28-disuccinate (DScB) (Fig. 1), with (2-hydroxypropyl)-γ-cyclodextrin was used as an example. Pentacyclic lupane triterpenoids, such as betulin and its derivatives, exhibit antitumor and other types of biological activities [45]. Previously, the interaction of a number of betulin derivatives (betulinic and betulonic acids, and sulphated betulin derivatives) with β-CD, (2-hydroxypropyl)-β-cyclodextrin and (2-hydroxypropyl)-γ-cyclodextrin (HP-β-CD, HP-γ-CD) has been studied [7-9, 46-48].

Experimental

Instrumentation

The CE measurements were performed using a diode-array detector Agilent 7100 (Agilent Technologies, Waldbronn, Germany) of the Krasnoyarsk Regional Center of Research Equipment of Federal Research Center “Krasnoyarsk Science Center SB RAS”. A fused silica capillary with 50 μm id and the total/effective lengths of 80.5/72 cm was obtained from Agilent Technologies. The capillary was thermostated at 25.00 ± 0.04 °C. The computer program OpenLab CDS ChemStation Edition C.01.08 was employed for data acquisition and processing. The separation was carried out by applying a voltage of + 30 kV to the capillary inlet. The wavelength for direct detection was 200 nm with a bandwidth of 10 nm, unless otherwise stated. The sample injections were performed hydrodynamically at a pressure of 50 mbar for 5 sec. For each sample and BGE composition, 3 to 5 replicate injections were made.

A new capillary was first rinsed with 1 M NaOH for 10 min, then with ultra pure water for 10 min. At the beginning of each day, the capillary was first rinsed with 0.1 M NaOH for 5 min, twice with ultra pure water for 10 min and with running BGE for 15 min. Between runs the capillary was rinsed with BGE for 5 min.

pH measurements were performed using a calibrated pH instrument «Expert-001-1» (Econix-Expert, Moscow, Russia).

Chemicals

The reagents of analytical grade purity were used. HP-γ-CD (a extent of labeling and an average relative molecular mass were 0.6 molar substitution and 1580, respectively) was

obtained from Sigma-Aldrich (Moscow, Russia). Dimethyl sulfoxide (DMSO) dissolved in samples with a concentration of 0.001 % was used as an electroosmotic flow (EOF) marker. Solutions were prepared using deionized water with electrical conductivity less than 0.1 μS·cm^{-1} obtained from a water purification system Direct-Q3 (Millipore, France). All solutions were filtered through 0.45 μm filters.

The ester betulin derivatives were synthesized in Institute of Chemistry and Chemical Technology SB RAS, Federal Research Center "Krasnoyarsk Science Center SB RAS" [49-51]. Stock compounds solutions with a concentration of 1 g/L were obtained by dissolution of accurate weights in BGE without the HP-γ-CD addition. Solutions of 10 mM disodium tetraborate decahydrate with pH 9.18 with the addition of 0 - 5000 μM HP-γ-CD were utilized as BGEs. For each electrophoretic separation on the base of a specific BGE containing HP-γ-CD, samples were prepared by dilution of the stock compounds solutions with this BGE.

Separation conditions and calculation

The effective electrophoretic mobility from experimental data was calculated using the following equations:

$$\mu_{eff,\ i} = \frac{l \cdot l_{eff}}{U}\left(\frac{1}{a_{1,i} - t_{corr}} - \frac{1}{t_{eof} - t_{corr}}\right) \quad (5)$$

$$t_{corr} = (t_{finish} - t_{start})/2 + t_{start} \quad (6)$$

where l and l_{eff} are the total and effective capillary lengths, respectively, U is the voltage, t_{corr} is the correction time taking into account the fact that the voltage is not applied instantly and not from zero time, t_{EOF} is the migration time of the EOF marker (neutral compound, dimethyl sulfoxide, DMSO); t_{start} is the time, starting from which the voltage is applied, t_{finish} is the time at which the voltage achieves the setting value (in our study, this times were 0.01 and 0.18 min, respectively).

The coefficient allowing the correction for the change in viscosity for each BGE, υ, was calculated as follows [7]:

$$\upsilon = t'/t^0 \quad (7)$$

where t' and t^0 are the times for the DMSO peaks obtained at a voltage of 0 kV and a pressure of 100 mbar in the BGEs with the HP-γ-CD addition and without it, respectively.

The binding constants for the 1:1 complexes with HP-γ-CD and ionic mobilities were calculated from the nonlinear regression fitting by minimizing the differences in viscosity corrected experimental and theoretical electrophoretic mobilities (Eqs. (1), (5) or Eq. (S3.1)). The fitting [9] was carried out using the CEval software (v.5.6.3, Prague, Czech Republic, http://echmet.natur.cuni.cz/ [29]) and OriginPro 8.1 (OriginLab Corporation, Northampton,

USA). Fitting the electrophoretic peaks with the HVL function was carried out using CEval and MS Excel.

Results and discussion

Determining binding constants

Electropherograms of ester betulin derivatives were recorded using BGEs with different HP-γ-CD content. It was found that the complexation is a high-affinity interaction and a mobility change occurs at a sufficiently low HP-γ-CD concentration (μM). The complexes studied are kinetically labile because no peaks of the complexes were observed in the electropherograms recorded using BGE without the HP-γ-CD addition (to obtain the complexes, HP-γ-CD was added to the samples as described in [47]). For this case, it is important to choose the lowest possible analyte concentration. Because triangular peaks are lower than the peaks recorded in BGE without the HP-γ-CD addition or with a high HP-γ-CD concentration, it was found that the signal-to-noise ratio (S/N) should be about 10 for BGE without HP-γ-CD. Peaks with S/N ~ 10 under sample injection at 50 mbar and 5 sec were found to be observed at DPhB and DScB concentrations equal to 2 and 70 μM, respectively, because of the lower molar absorbance of succinate compared to the one corresponding to phthalate. Electropherograms of the ester betulin derivatives at these concentrations were recorded using BGEs with different HP-γ-CD content. Fig. 2 shows examples of the obtained electropherograms. In the rectangles in Fig. 2, examples of peaks fitted with the HVL function are presented; the vertical dotted lines indicate the migration time corresponding to the parameter a_1 of the HVL function.

Peaks obtained with BGEs containing 0.05 μM HP-γ-CD and lower for DPhB and lower than 2.0 μM HP-γ-CD for DScB had a corrupted triangular shape (Fig. 3) and were not fitted with the HVL function. Such data were not used in further calculations. It follows that the permissible excess of analyte concentration over ligand concentration is approximately 30 times on condition that the parameter a_1 of the HVL function is used to calculate the effective electrophoretic mobility. But this conclusion concerns samples obtained by dilution using BGE with the ligand addition, that is, for samples for which the stacking effects are eliminated. Since, at present time, there is no true correction of the stacking effects on the effective electrophoretic mobility for ms ACE data.

Electrophoretic mobilities of DPhB and DScB (Fig. 4a, b) were calculated using the parameter a_1 of the HVL function (Eq. (5)), and binding constants were calculated. The binding constant logarithms, designated as log $K_{11}(a_1)$, and the 95 % confidence intervals at 25 °C obtained from the CEval software and OriginPro8.1 are shown in Table 1. As can be seen from Table 1, the results obtained by the two software are in good agreement, and the constants values are equal within error. The electrophoretic mobilities μ_D and μ_{11} are -21.1 ± 0.1 and -13.77 ±

0.05 10^{-9} m^2 V^{-1} s^{-1} for DPhB and -22.99 ± 0.07 and -14.20 ± 0.03 10^{-9} m^2 V^{-1} s^{-1} for DScB, respectively. As can be seen from Fig. 4a, b and Electronic Supplementary Material, section S2, the obtained experimental data on electrophoretic mobilities well agree with the theoretical curves for 1:1 complexes and don't match the theoretical curves for 1:2 complexes.

Comparison of Fig. 4a with Fig. 4b shows that there are considerably fewer points for DScB than for DPhB. As mentioned above, this is caused by the fact that the peaks had a corrupted triangular shape when the ratio of analyte concentration in samples to ligand concentration in BGE was higher than 30-35 times and the fact that the peaks with S/N ~ 10 were observed for 2 μM DPhB and 70 μM DScB. That is, we cannot decrease the DScB concentration to obtain more experimental points. The DPR values calculated from Eq. (2) are 0.44 for DPhB and only 0.04 for DScB; this results in a more than 3 times larger error for DScB in the binding constants value.

Errors in binding constants obtained from the mobility calculated from the peak apex time

Table 1 shows a comparison of binding constant logarithms obtained from the mobilities calculated using the parameter a_1 of the HVL function and using the migration time measured at the peak apex, designated as log $K_{11}(a_1)$ and log $K_{11}(t_{max})$, respectively. Calculation details are described in Electronic Supplementary Material, section S3. As can be seen from Table 1, the values of log $K_{11}(t_{max})$ are understated by 0.4-0.5 logarithmic units relative to log $K_{11}(a_1)$, and 95 % CIs don't overlap. For non-logarithmic units, the underestimation relative to $K_{11}(a_1)$ is 50-70 %. In addition, for DPhB, besides the significant systematic error, a significant random error is observed, CI is almost 5 times wider. Fig. 4c, d shows the experimental points calculated from the peak apex time and theoretical curves drawn using Eq. (1) with $K_{11}(t_{max})$ and ionic mobilities found by the nonlinear regression fitting for this case. It is worth noting that the experimental random error in determining the mobility (0.3-0.7 %) is comparable to the size of the experimental points in Fig. 4c, d or lower than the size. Thus, Fig. 4c, d shows that Eq. (1) is unable to describe the position of experimental points for DPhB; for DScB, this is not so obvious due to fewer points.

The difference in situations for DPhB and DScB is also associated with fewer points for DScB. In connection with this fact, it is interesting how the calculated values of log $K_{11}(t_{max})$ changes if the HP-γ-CD concentration range in BGE is narrowed due to removal of the lowest (nonzero) concentrations. Table 2 shows these values along with 95 % CIs and its width. For cases 4-6, as seen from Table 2 and Fig. S3.1, 95 % CIs overlap with CIs for log $K_{11}(a_1)$, and the discrepancy between the experimental points and theoretical curves is almost within error. While for cases 1-3, this discrepancy is still significant (Fig. S3.1). But for cases 4-6, CIs are 2-4 times

wider than those for log $K_{11}(a_1)$. Firstly, this is due to the fact that the peaks at a HP-γ-CD concentration of 0.5 μM and higher are still slightly triangular; secondly, a narrow range of changing the mobility from the value for the lowest (nonzero) concentration HP-γ-CD concentration to the complex mobility (narrow DPR) results in wider CI widths because of an significant effect of the experimental random error of determining mobility near the plateau of the biding curve (as for log $K_{11}(a_1)$ of DScB). The decrease in peak triangularity with an increase HP-γ-CD concentration in BGE (Fig. 2A) causes a decrease in the CI width in the sequence of cases 1-4 in Table 2. While narrowing the HP-γ-CD concentration range leads to broadening the CI width in the sequence of cases 4-6. Table S3.2 shows that the results from OriginPro 8.1 is comparable within error to the results from CEval software. It is worth noting that the 95 % CI values for log $K_{11}(a_1)$ for cases 1-6 overlap each other (Table S3.3); for cases 1-3, the CI widths are practically the same, while in the sequence of cases 4-6, this width increases for the same reason as the width for log $K_{11}(t_{max})$. For all cases 1-6 for log $K_{11}(a_1)$, the theoretical curves and experimental points agree within error (Fig. S3.2).

Thus, using the peak apex time for triangular peaks in mobility calculation and the subsequent calculation of binding constants results in systematic and random errors, whose values are determined by how wide the triangular peaks are (this, in turn, depends on the ligand concentration range in BGE and analyte concentration in samples).

Effect of analyte concentration

Then the effect of increasing the analyte concentration in samples on the peak position, peak shape and value of the parameter a_1 of the HVL function was studied at a fixed ligand concentration in BGE. DPhB is well suited for this study due to the presence of two benzene rings having good absorption in UV region and the fact that this compound can be recorded in electropherograms at a concentration of μM level. A BGE with 1 μM HP-γ-CD content was chosen. For this BGE, 94 % analyte, as follows from Eq. (3), should be in the complexed form at an infinite dilution concentration of the analyte. Electropherograms of DPhB with different concentration were recorded using this BGE (Fig. 5). Here, additional detection was performed at 230 nm to obtain peaks with a lower S/N ratio because the analyte is injected with a concentration as small as possible when the strong complexation is studied and the S/N ratio is usually low for such case. As can be seen from Fig. 5, the decrease of peak symmetry is observed with increasing analyte concentration. For r = 20 and 30 ($r = C_{an}/C_L$), dips on the stretched side of the peaks appear and this peak side consists of two nonparallel lines. The obtained peaks were fitted with the HVL function by CEval software. In Fig. 5, the migration times corresponding to the parameter a_1 of the HVL function are shown by the vertical dotted lines. The parameter a_1 shifts toward higher migration times with increasing analyte

concentration, while the DMSO peak position is constant. The deviation of the effective electrophoretic mobility obtained using the parameter a_1 for r = 10 from the values for r = 2 is 0.7 %. This is comparable to the experimental random error in determining the mobility (0.3-0.7 %). But the deviation of the effective electrophoretic mobility obtained using the parameter a_1 for r = 20 from those for r = 2 is already 2.7 %, which is considerably higher than the experimental error in determining the mobility. In addition, the peaks with the dips fit to the HVL function with a deviation exceeding the baseline fluctuations as this function is not intended for peaks with such disturbances. For the peaks at r = 30, CEval software draws incorrectly the baseline using automatically set-up parameters, and only about half of the peaks is fitted with HVL function. In addition, as can be seen from Fig. 5, the peak at r = 30 is located beyond the time borders of the peak at r = 2. Thus, as follows from these experiments, it is permissible to use no more than 10-fold excess of the analyte concentration in samples over the ligand concentration in BGE, provided that the peaks are fitted with the HVL function.

However, the obtained results pertain to a particular compound (DPhB) at a concentration of 2 μM in BGE with 1 μM HP-γ-CD. In practice, as can be seen from Fig. 3a, the DPhB peak is still triangular without distortion at a HP-γ-CD concentration of 0.075 μM (r = 27), which is probably related to the fact that only 56 % analyte is in a complexed form at this HP-γ-CD concentration. The DScB peak (Fig. 3b) is still triangular without distortion at a HP-γ-CD concentration of 2.0 μM (r = 35, R = 0.96), which is probably due to higher concentrations of DScB and HP-γ-CD. If mobilities obtained from the disturbed triangular peaks with dips are used in calculation of binding constants (via the parameter a_1 at HP-γ-CD concentrations of 0.01, 0.025 and 0.05 μM for DPhB and 0.5, 1 and 2 μM for DscB), then the calculated values of these constants are biased, and the deviation of theoretical values from experimental ones reaches 2.9 % for DPhB and 2.5 % for DScB; this exceeds the experimental random error in determining mobility, 0.3-0.7 %. Therefore, the disturbed triangular peaks should not be used in the calculations. Thus, a 10-35 fold excess of the analyte concentration in the samples over the ligand concentration in BGE can be considered as a tentative limit, but the peak shape should ultimately be a landmark. The lower the analyte concentration, the lower the ligand concentration in BGE that can be used. In connection with this and the fact that a narrow range of mole fractions of the complexed analyte (narrow DPR) due to a narrow range of HP-γ-CD concentration leads to low precision of the calculated values of binding constants (Tables 2, S3.2, and S3.3), the lowest possible analyte concentration should be used.

The appearance of the dip in the peaks can be explained as follows. In the sample zone for which the equilibrium ratio of the complex concentration to the analyte concentration has not yet been achieved, the ligand is being consumed on the complex formation during the ligand

movement through the sample zone. If the ligand concentration in BGE is too low, then it may be that the ligand is sufficient only for part of the zone in the initial time after voltage application. This leads to the formation of the dip in the peak. The dip formed in the beginning remains during subsequent electrophoretic separation. The presence of the dip probably depends on the value of binding constant, ligand concentration in BGE, sample length, electrophoretic and ionic mobilities, and some other parameters. The observed mobility of such distorted peaks deviates from the theoretical mobility. As examples, Fig. 2a (curve for 0.025 μM HP-γ-CD) and Fig. 2b (curves for 0.5 and 1 μM HP-γ-CD) illustrate that the position of the peaks is remote from the expected migration times indicated by solid lines.

Comparing binding constants for the CD complexes of betulin derivatives

Table 3 shows a comparison of the obtained binding constants with the data available in the literature for the CD complexes of betulin derivatives in aqueous solutions at 25 °C. As can be seen from Table 3, the highest binding constants are observed for the HP-γ-CD complexes. The values of the logarithms are 2-3 units higher compared to those for the β-CD and HP-β-CD complexes. This is possibly due to the larger size of the molecule (γ-CD and β-CD consist of 8 and 7 glucose residues, respectively). In addition, stabilization of the HP-β-CD and HP-γ-CD inclusion complexes can occur due to hydrophobic interactions of the compounds with alkyl chains of 2-hydroxypropyl groups. This is, the alkyl chains increase the hydrophobic cavity in the host molecule. The water-insoluble betulin derivatives (BIA and BOA) form less stable complexes with CDs as compared to other derivatives. This is possibly caused by a larger number of hydrogen bonds between sulfonate, carboxylic and acetate groups of other betulin derivatives and hydroxyl or hydroxypropyl groups of CDs. Table 3 also shows that the values of binding constants of the HP-γ-CD complexes for DPhB, DScB and ASB are almost equal within error, while those for DSB is slightly lower. This is probably due to the fact that DPhB and DScB contain two phthalate and succinate groups at opposite ends of the molecule (Fig. 1a), respectively. The groups are known to have an affinity to the hydrophobic cavity of CDs [21, 40], this creates light steric hindrances for the complex dissociation and leads to higher binding constants. ASB containing relatively compact acetic and sulfonate groups is a singly charged ion in solution, while DPhB, DScB and DSB are doubly charged ions, and a decrease in the guest charge usually leads to increasing binding constants [8].

Conclusions

The features of using mobility shift affinity capillary electrophoresis for studying the strong complexation were discussed. Complexes between (2-hydroxypropyl)-γ-cyclodextrin and betulin 3,28-diphthalate and betulin 3,28-disuccinate were used as an example. Since the complexation is strong, a very low amount of HP-γ-CD was added to the BGE, and the triangular

peaks appeared. It was shown that, in order to minimize the systematic and random errors, the effective electrophoretic mobility for such peaks should be calculated using the parameter a_1 of the HVL function instead of the migration time measured at the peak apex. The effect of analyte concentration in samples as compared to ligand concentration in BGE on the peaks shape and the parameter a_1 of the HVL function was studied. The permissible excess of analyte concentration over ligand concentration was found to be about 10-35-fold, provided that the parameter a_1 of the HVL function is used and the samples are obtained by dilution using BGEs. It was shown that disturbed triangular peaks with dips were observed with a greater excess of analyte concentration over ligand concentration and these peaks should not be used in calculations because of significant shifting. It follows that the lowest possible analyte concentration (with S/N ~ 10) should be used. This allows using a wider range of ligand concentration providing a wider range of mole fractions of the complexed analyte (wider DPR) and it leads to higher precision in determining the values of binding constants. The observed features were found at the first time for guest-host type interactions and were not reported for other types of intermolecular interactions with fast on-off kinetics such as drug-protein, drug-nucleic acid, protein-nucleic acid, etc.

The calculated values of the binding constants logarithms at 25 °C are 7.23 ± 0.03 and 7.13 ± 0.10 for the 1:1 complexes of DPhB and DScB with HP-γ-CD, respectively. The obtained values of binding constants were compared with the values for the CD complexes of different betulin derivatives. The binding constants of the HP-γ-CD complexes were shown to be higher by a factor of 100-1000 than to the binding constants of the β-CD and HP-β-CD complexes.

Declarations

Funding information This work was conducted within the framework of the budget project AAAA-A17-117021310221-7 for Institute of Chemistry and Chemical Technology SB RAS.

Compliance with ethical standards

Conflict of interest The authors declare that they have no conflict of interest.

References

1. Crini G. Review: a history of cyclodextrin. Chem Rev. 2014;114:10940–75.
2. Jacob S, Nair AB. Cyclodextrin complexes: perspective from drug delivery and formulation. Drug Dev Res. 2018;79:201–17.
3. Mura P. Analytical techniques for characterization of cyclodextrin complexes in aqueous solution: a review. J Pharm Biomed Anal. 2014;101:238–50.

4. Olabi M, Stein M, Wätzig H. Affinity capillary electrophoresis for studying interactions in life sciences. Methods. 2018;146:76–92.
5. Dubský P, Dvořák M, Ansorge M. Affinity capillary electrophoresis: the theory of electromigration. Anal Bioanal Chem. 2016;408:8623–41.
6. Musile G, Cenci L, Andreetto E, Ambrosi E, Tagliaro F, Bossi AM. Screening of the binding properties of molecularly imprinted nanoparticles via capillary electrophoresis. Anal Bioanal Chem. 2016;408:3435–43.
7. Popova OV, Sursyakova VV, Burmakina GV, Levdansky VA, Rubaylo AI. Determination of stability constants of inclusion complexes of betulin derivatives with β-cyclodextrin by capillary electrophoresis. Dokl Chem. 2015;461:67–9.
8. Sursyakova VV, Levdansky VA, Rubaylo AI. Thermodynamic parameters for the complexation of water-soluble betulin derivatives with (2-hydroxypropyl)-β-cyclodextrin determined by affinity capillary electrophoresis. J Mol Liq. 2019;283:325–31.
9. Sursyakova VV, Levdansky VA, Rubaylo AI. Strong complexation of water-soluble betulin derivatives with (2-hydroxypropyl)-γ-cyclodextrin studied by affinity capillary electrophoresis. Electrophoresis. 2020;41:112–5.
10. Stein M, Haselberg R, Mozafari-Torshizi M, Wätzig H. Experimental design and measurement uncertainty in ligand binding studies by affinity capillary electrophoresis. Electrophoresis. 2019;40:1041–54.
11. Pangavhane S, Makrlík E, Ruzza P, Kašička V. Affinity capillary electrophoresis employed for determination of stability constants of antamanide complexes with univalent and divalent cations in methanol. Electrophoresis. 2019;40:2321–8.
12. Nevídalová H, Michalcová L, Glatz Z. Capillary electrophoresis-based approaches for the study of affinity interactions combined with various sensitive and nontraditional detection techniques. Electrophoresis. 2019;40:625–42.
13. Neaga IO, Hambye S., Bodoki E., Palmieri C, Ansseau E, Belayew A, Oprean R, Blankert B. Affinity capillary electrophoresis for identification of active drug candidates in myotonic dystrophy type 1. Anal Bioanal Chem. 2018;410:4495–507.
14. Neaga IO, Hambye S., Bodoki E., Palmieri C, Eynde JJV, Ansseau E, Belayew A, Oprean R, Blankert B. Correction to: Affinity capillary electrophoresis for identification of active drug candidates in myotonic dystrophy type 1. Anal Bioanal Chem. 2019;411:545.
15. Ansorge M, Dubský P, Ušelová K. Into the theory of the partial-filling affinity capillary electrophoresis and the determination of apparent stability constants of analyte-ligand complexes. Electrophoresis. 2018;39:742–51.

16. Konášová R, Koval D, Jaklová Dytrtová J, Kašička V. Comparison of two low flow interfaces for measurement of mobilities and stability constants by affinity capillary electrophoresis–mass spectrometry. J Chromatogr A. 2018;1568:197–204.
17. Aizpurua-Olaizola O, Torano JS, Pukin A, Fu O, Boons GJ, de Jong GJ, Pieters RJ. Affinity capillary electrophoresis for the assessment of binding affinity of carbohydrate-based cholera toxin inhibitors. Electrophoresis. 2018;39:344–7.
18. Kanizsová L, Ansorge M, Zusková I, Dubský P. Using single-isomer octa(6-O-sulfo)-cyclodextrin for fast capillary zone electrophoretic enantioseparation of pindolol: Determination of complexation constants, software-assisted optimization, and method validation. J Chromatogr A. 2018;1568:214–21.
19. Mofaddel N, Fourmentin S, Guillen F, Landy D, Gouhier G. Ionic liquids and cyclodextrin inclusion complexes: limitation of the affinity capillary electrophoresis technique. Anal Bioanal Chem. 2016;408:8211–20.
20. Holm R, Hartvig RA, Nicolajsen HV, Westh P, Østergaard J. Characterization of the complexation of tauro and glyco-conjugated bile salts with γ-cyclodextrin and 2-hydroxypropyl-γ-cyclodextrin using affinity capillary electrophoresis. J Incl Phenom Macrocycl Chem. 2008;61:161–9.
21. Sursyakova VV, Rubaylo AI. Stability constants of adducts of succinate copper(II) complexes with β-cyclodextrin determined by capillary electrophoresis. Electrophoresis. 2018;39:1079–85.
22. Pangavhane S, Böhm S, Makrlík E, Ruzza P, Kašička V. Affinity capillary electrophoresis and quantum mechanical calculations applied to investigation of [Gly^6]-antamanide binding with sodium and potassium ions. Electrophoresis. 2017;38:1551–9.
23. Sursyakova VV, Burmakina GV, Rubaylo AI. Composition and stability constants of copper(II) complexes with succinic acid determined by capillary electrophoresis. J Coord Chem. 2017;70:431-40.
24. Tůmová T, Monincová L, Čeřovský V, Kašička V. Estimation of acidity constants, ionic mobilities and charges of antimicrobial peptides by capillary electrophoresis. Electrophoresis. 2016;37:3186–95.
25. Sursyakova VV, Burmakina GV, Rubaylo AI. Influence of analyte concentration on stability constant values determined by capillary electrophoresis. J Chromatogr Sci. 2016;54:1253–62.
26. Sladkov V. Affinity capillary electrophoresis in studying the complex formation equilibria of radionuclides in aqueous solutions. Electrophoresis. 2016;37:2558–66.

27. Ehala S, Kašička V, Makrlík E. Determination of stability constants of valinomycin complexes with ammonium and alkali metal ions by capillary affinity electrophoresis. Electrophoresis. 2008;29:652–7.
28. Jiang C, Armstrong DW. Use of CE for the determination of binding constants. Electrophoresis. 2010;31:17–27.
29. Dubský P, Ördögová M, Malý M, Riesová M. CEval: All-in-one software for data processing and statistical evaluations in affinity capillary electrophoresis. J Chromatogr A. 2016;1445:158–65.
30. Šlampová A, Malá Z, Gebauer P. Recent progress of sample stacking in capillary electrophoresis (2016–2018). Electrophoresis. 2019;40:40–54.
31. Vespalec R, Boček P. Calculation of stability constants for the chiral selector–enantiomer interactions from electrophoretic mobilities. J Chromatogr A. 2000;875:431–45.
32. Hruška V, Svobodová J, Beneš M, Gaš B. A nonlinear electrophoretic model for PeakMaster: Part III. Electromigration dispersion in systems that contain a neutral complex-forming agent and a fully charged analyte. Theory. J Chromatogr A. 2012;1267:102–8.
33. Svobodová J, Beneš M, Hruška V, Ušelová K, Gaš B. Simulation of the effects of complex-formation equilibria in electrophoresis: II. Experimental verification. Electrophoresis. 2012;33:948–57.
34. Beneš M, Svobodová J, Hruška V, Dvořák M, Zusková I, Gaš B. A nonlinear electrophoretic model for PeakMaster: Part IV. Electromigration dispersion in systems that contain a neutral complex-forming agent and a fully charged analyte. Experimental verification. J Chromatogr A. 2012;1267:109–15.
35. Galbusera C, Thachuk M, De Lorenzi E, Chen DDY. Affinity capillary electrophoresis using a low-concentration additive with the consideration of relative mobilities. Anal Chem. 2002;74:1903–14.
36. Le Saux T, Varenne A, Gareil P. Peak shape modeling by Haarhoff-Van der Linde function for the determination of correct migration times: a new insight into affinity capillary electrophoresis. Electrophoresis. 2005;26:3094–104.
37. Dubský P, Dvořák M, Műllerová L, Gaš B. Determination of the correct migration time and other parameters of the Haarhoff–van der Linde function from the peak geometry characteristics. Electrophoresis. 2015;36:655–61.
38. Erny GL, Bergström ET, Goodall DM. Electromigration dispersion in capillary zone electrophoresis. Experimental validation of use of the Haarhoff–Van der Linde function. J Chromatogr A. 2002;959:229–39.

39. Erny GL, Bergström ET, Goodall DM. Predicting peak shape in capillary zone electrophoresis: a generic approach to parametrizing peaks using the Haarhoff-Van der Linde (HVL) function. Anal Chem. 2001;73;4862–72.
40. Rekharsky MV, Inoue Y. Complexation thermodynamics of cyclodextrins. Chem Rev. 1998;98:1875–917.
41. Connors KA. The stability of cyclodextrin complexes in solution. Chem Rev. 1997;97:1325–58.
42. Holm R, Nicolajsen HV, Hartvig RA, Westh P, Østergaard J. Complexation of tauro- and glyco-conjugated bile salts with three neutral β-CDs studied by ACE. Electrophoresis. 2007:28;3745–52.
43. François Y, Varenne A, Sirieix-Plenet J, Gareil P. Determination of aqueous inclusion complexation constants and stoichiometry of alkyl(methyl)-methylimidazolium-based ionic liquid cations and neutral cyclodextrins by affinity capillary electrophoresis. J Sep Sci. 2007:30;751–60.
44. Le Saux T, Varenne A, Perreau F, Siret L, Duteil S, Duhau L, Gareil P. Determination of the binding parameters for antithrombin–heparin fragment systems by affinity and frontal analysis continuous capillary electrophoresis. J Chromatogr A. 2006;1132:289–96.
45. Tolstikova TG, Sorokina IV, Tolstikov GA, Tolstikov AG, Flekhter OB. Biological activity and pharmacological prospects of lupane terpenoids: I. natural lupane derivatives. Rus J Bioorg Chem. 2006;32:37–49.
46. Popova OV, Sursyakova VV, Burmakina GV, Maksimov NG, Levdansky VA, Rubaylo AI. Solubility study of betulonic acid in the presence of hydroxypropyl-γ-cyclodextrin by capillary electrophoresis. J Sib Fed Univ. Chem. 2016;9:171–6.
47. Sursyakova VV, Maksimov NG, Levdansky VA, Rubaylo AI. Combination of phase-solubility method and capillary zone electrophoresis to determine binding constants of cyclodextrins with practically water-insoluble compounds. J Pharm Biomed Anal. 2018;160:12–8.
48. Sursyakova VV, Levdansky VA, Rubaylo AI. Thermodynamic parameters for the complexation of water-insoluble betulin derivatives with (2-hydroxypropyl)-γ-cyclodextrin determined by phase-solubility technique combined with capillary zone electrophoresis. Electrophoresis. 2019;40:1656–61.
49. Levdanskii VA, Levdanskii AV, Kuznetsov BN. Synthesis of betulin dibenzoate and diphthalate. Chem Nat Compound. 2017;53:310–1.
50. Levdanskii VA, Levdanskii AV, Kuznetsov BN. Method for producing betulinol diphtalate. Russ Patent. RUS № 2614149. 23.03.2017.

51. Levdanskii VA, Levdanskii AV, Kuznetsov BN. Method of producing betulinol disuccinate. Russ Patent. RUS № 2638160. 12.12.2017.

Tables

Table 1 Binding constants obtained from the mobilities calculated using the parameter a_1 of the HVL function and using the migration time measured at the peak apex, t_{max}. In brackets, the 95 % CI is shown

Name	Log $K_{11}(a_1)$	Log $K_{11}(t_{max})$
	CEval software	
DPhB	7.23 ± 0.03*	6.86*
	(7.20-7.26)	(6.72-6.99)
DScB	7.13*	6.63*
	(7.05-7.24)	(6.55-6.72)
	OriginPro 8.1	
DPhB	7.23 ± 0.03	6.86*
	(7.20-7.26)	(6.67-6.99)
DScB	7.13 ± 0.10	6.63 ± 0.08
	(7.03-7.23)	(6.54-6.70)

* CI isn't shown after "±" because the interval are asymmetric relative to the mean

Table 2 Comparison of the binding constants, 95 % CIs (calculated by CEval software) and widths of the 95 % CI obtained from mobilities calculated using the migration time measured at the peak apex for different ranges of HP-γ-CD concentration (different DPR ranges). The 95 % CI for log $K_{11}(a_1)$ for 0.075-5000 μM concentration range of HP-γ-CD is 7.20-7.26

№	Sign in Fig. S3.1	HP-γ-CD concentration, μM	DPR[a]	Log $K_{11}(t_{max})$	95 % CI	w(95 % CI)[b]
1	a	0.075-5000	0.44	6.86	6.72-6.99	0.27
2	b	0.1-5000	0.37	6.90	6.77-7.03	0.26
3	c	0.25-5000	0.19	7.03	6.94-7.12	0.18
4	d	0.5-5000	0.11	7.17	7.11-7.25	0.14
5	e	0.75-5000	0.07	7.23	7.15-7.33	0.18
6	f	1-5000	0.06	7.28	7.18-7.43	0.25

[a] DPR was calculated using Eqs. (2), (3) and log $K_{11}(a_1)$ = 7.23

[b] The width of the 95 % CI was calculated as the difference between the upper and lower CI limits, Eq. (S3.3)

Table 3 Comparison of the obtained binding constants with the data available in the literature for CD complexes of betulin derivatives in aqueous solutions at 25 °C. The 95% CI is shown after «±». DSB, betulin 3,28-disulfate; ASB, betulin 3-acetate-28-sulfate; BIA, betulinic acid; BOA, betulonic acid

Name	Log K_{11}		
	β-CD	HP-β-CD	HP-γ-CD
DPhB	-[a]	-	7.23 ± 0.03
DScB	-	-	7.13 ± 0.10
DSB	3.87 ± 0.01 [7]	4.56 ± 0.01 [8]	6.70 ± 0.05 [9]
ASB	4.00 ± 0.02 [7]	4.96 ± 0.04 [8]	7.03 ± 0.10 [9]
BIA	2.40 ± 0.04 [7]	-[b][47]	3.82 ± 0.12 [47]
BOA	2.48 ± 0.03 [7]	-[b][47]	3.88 ± 0.14 [47]

[a] The complexes binding constants are not determined

[b] The complexes are not stable enough or they are formed very slowly

Figures

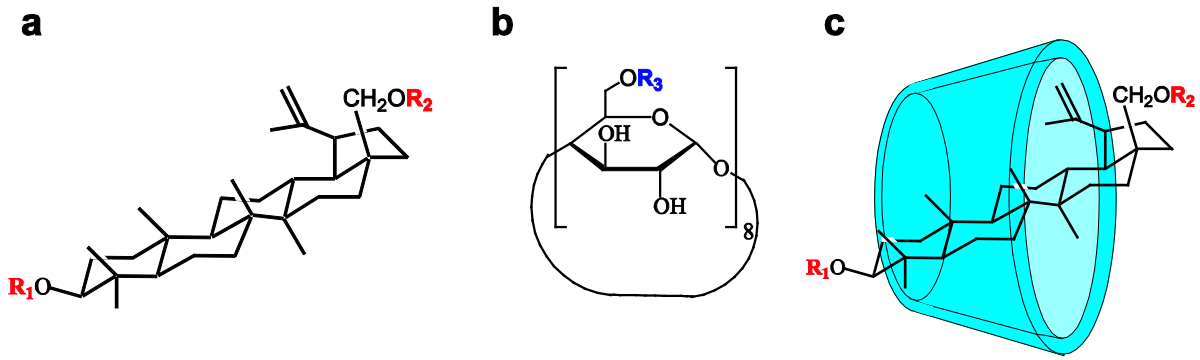

Fig. 1 (a) Structural formulas of ester betulin derivatives studied, (b) HP-γ-CD, and (c) possible scheme of inclusion complexes of betulin derivatives with HP-γ-CD. R_1, R_2 = -COC_6H_4COOH for betulin 3,28-di-ortho-phthalate, R_1, R_2 = -$COCH_2CH_2COOH$ for betulin 3,28-disuccinate, R_3 = H or –$CH_2CHOHCH_3$ (average degree of substitution is 0.6)

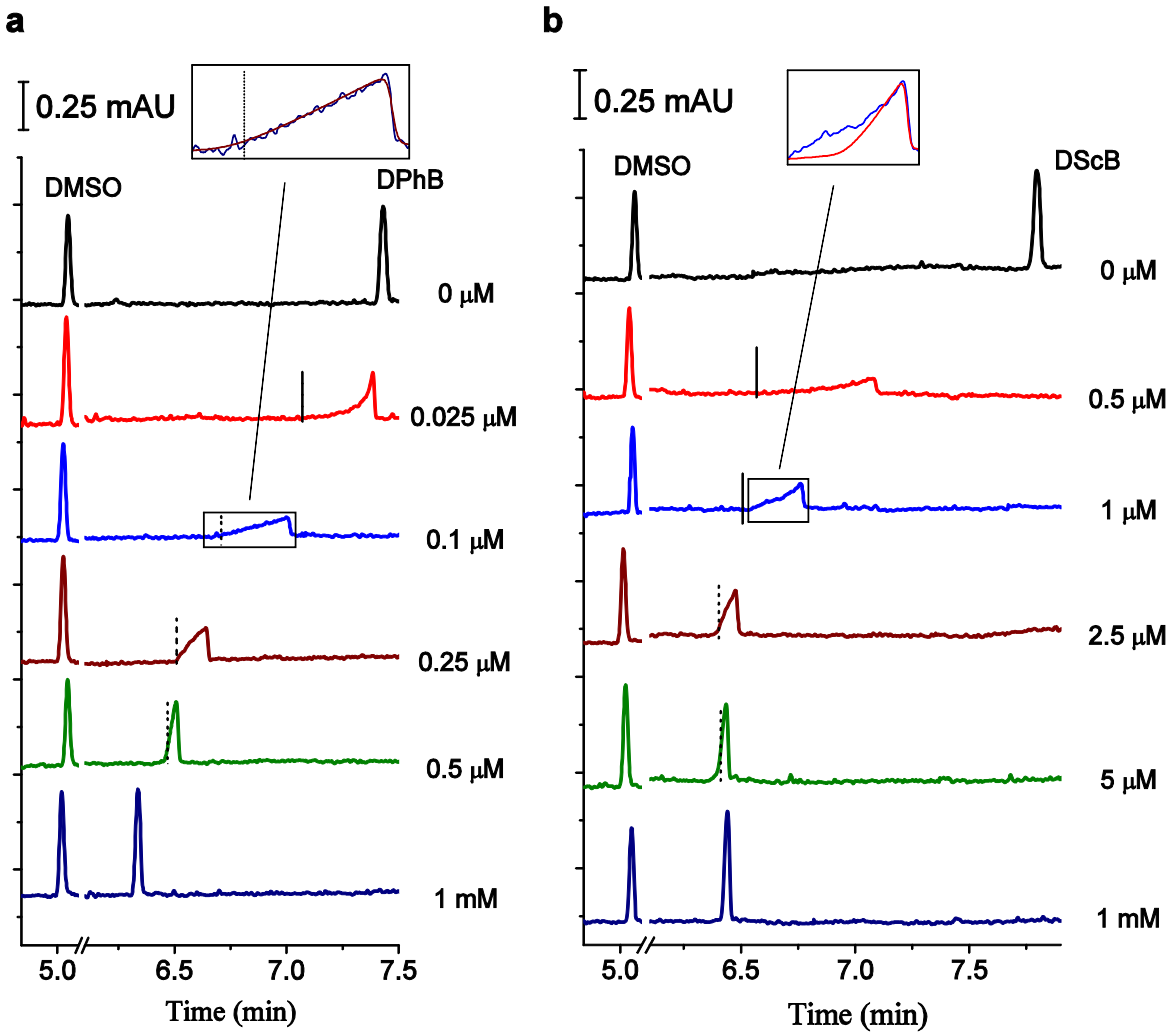

Fig. 2 Effect of the HP-γ-CD concentration in BGE on the shape and position of the (a) DPhB and (b) DScB electrophoretic peaks. The DPhB and DScB concentrations were 2 and 70 µM, respectively. In rectangles, the peaks fitted with the HVL function are shown. The vertical dotted lines indicate the migration time corresponding to the parameter a_1 of the HVL function. The vertical solid lines for 0.025 µM (a) and 0.5 and 1 µM (b) concentrations indicate the theoretical migration time for the DPhB and DScB peaks, respectively

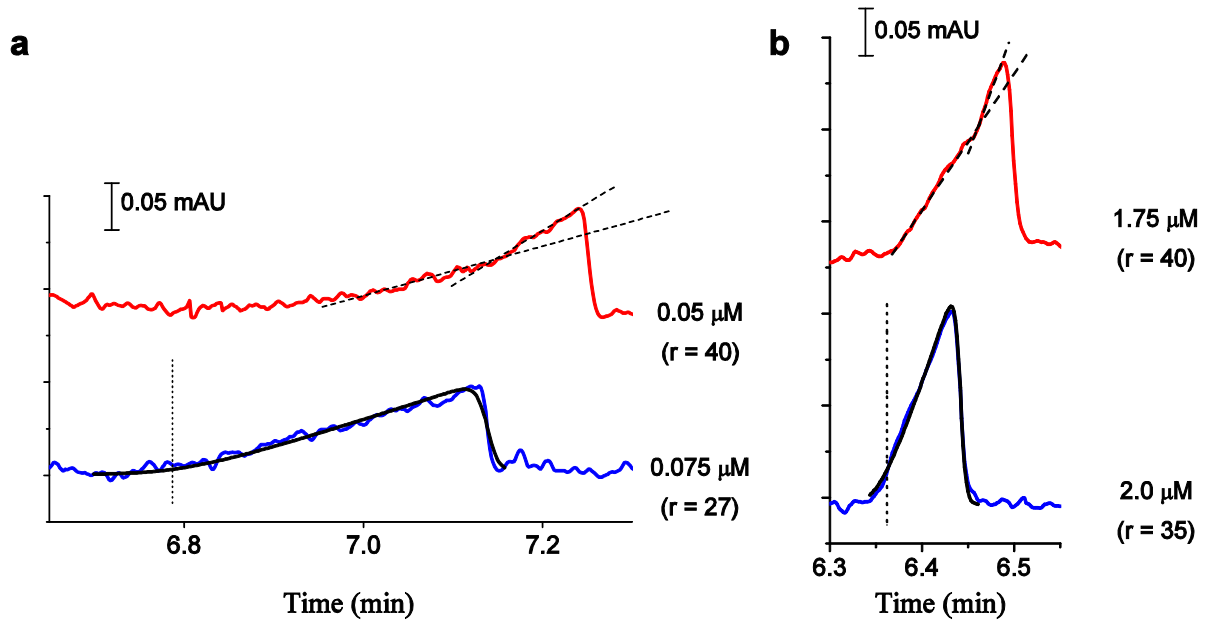

Fig. 3 Electrophoretic peaks of (a) DPhB and (b) DScB obtained using BGEs with such HP-γ-CD concentrations at which the peaks cannot yet be fitted with the HVL function and can already be fitted with the HVL function (the upper and bottom signals, respectively). The vertical dotted lines indicate the migration time corresponding to the parameter a_1 of the HVL function. Crossing dashed lines indicate a disturbed form of the peaks. The DPhB and DScB concentrations were 2 and 70 μM, respectively

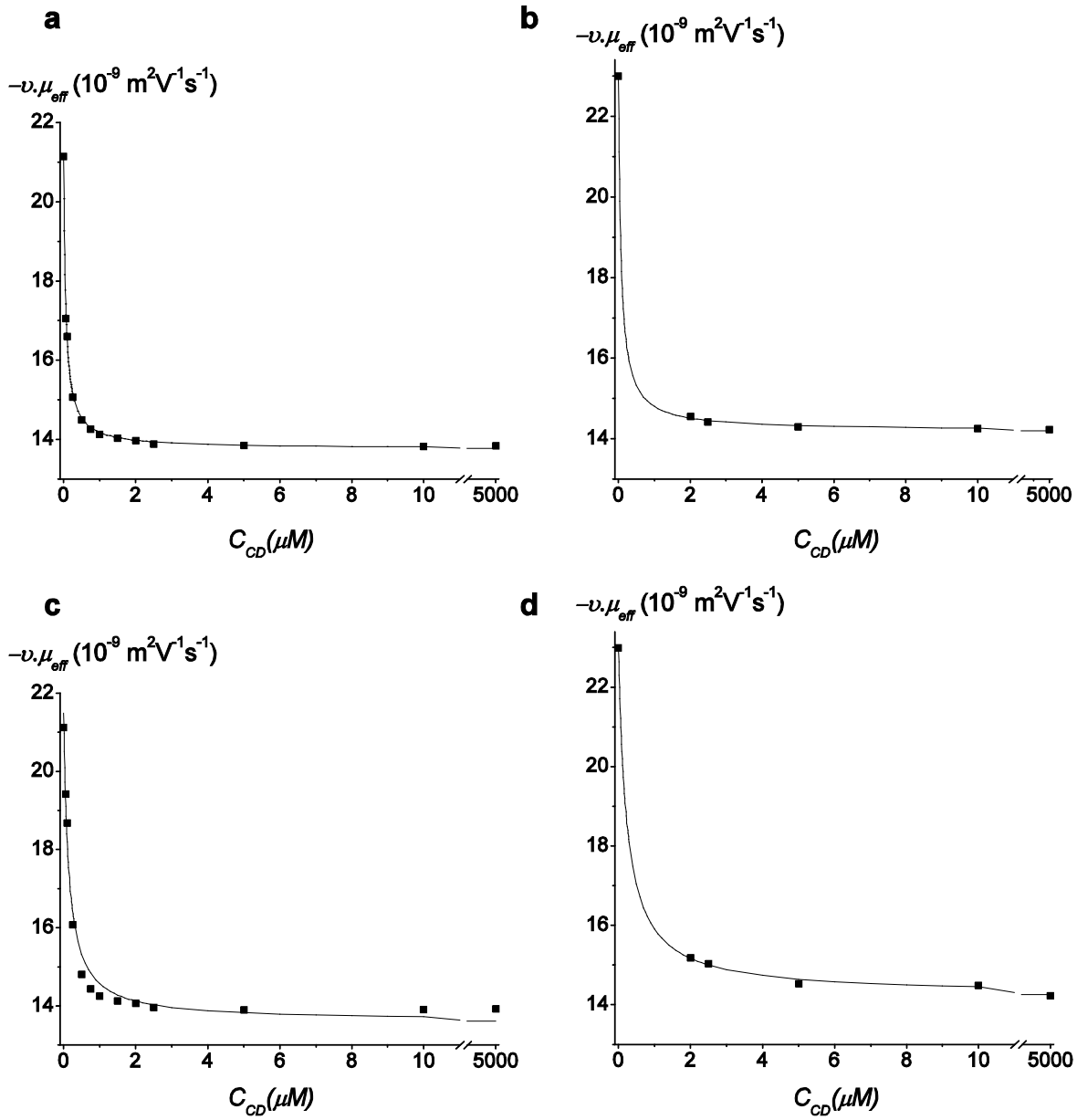

Fig. 4 Dependences of the viscosity corrected electrophoretic mobility of (a, c) DPhB and (b, d) DScB on the HP-γ-CD concentration in BGE. The mobility was calculated using (a, b) the parameter a1 of the HVL function for asymmetrical peaks and (c, d) the migration time measured at the peak apex. The points are experimental values and the curves are theoretically drawn using Eq. (1) on the base of binding constants and ionic mobilities calculated from the nonlinear regression fitting by minimizing the differences in viscosity corrected experimental and theoretical electrophoretic mobilities

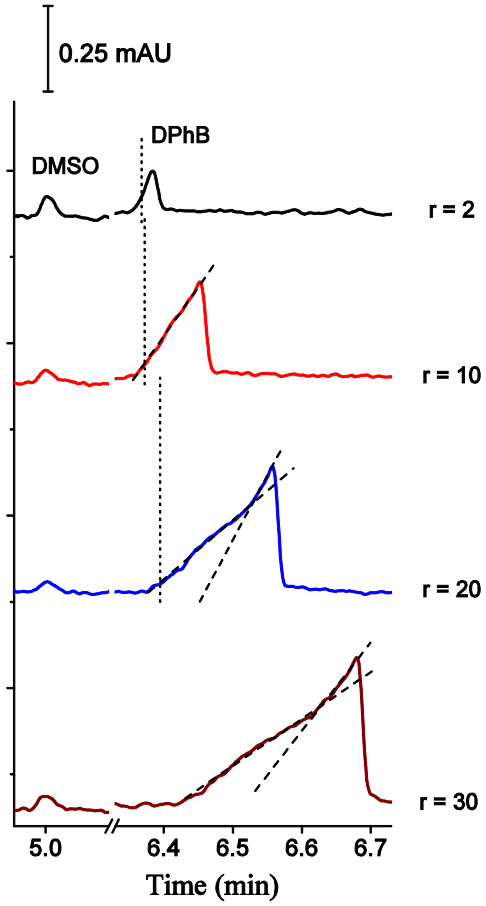

Fig. 5 Effect of the ratio of the DPhB concentration in the sample to the HP-γ-CD concentration in BGE (r) on the shape and position of the DPhB peak. The HP-γ-CD concentration in BGE was 1 μM, the DPhB concentration was 2-30 μM. The direct detection was made at 230 nm. The mole fraction of DPhB bound in complex was 94 %. The vertical dotted lines indicate the migration time corresponding to the parameter a_1 of the HVL function (obtained by CEval). Crossing dashed lines indicate a disturbed form of the peaks

Graphical abstract (for Table of contents)